LARGE SCALE TESTS FOR THE HYSTERESIS BEHAVIOR OF INCLINED BRACING MEMBERS

Heinrich Gugerli[I] and Subhash C. Goel[II]

SUMMARY

Tests were performed on diagonally mounted steel bracing members to investigate the response to cyclic displacements in the inelastic range. The members have a length of 141 in. (358 cm) and the connections are fully welded. Three cold-formed structural tubes and one hot-rolled wide-flange shape were tested with slenderness ratio ℓ/r ranging from 80 to 180. All specimens buckled in a symmetric mode with plastic hinges at the ends and midspan. The results are very similar to those obtained by previous investigators by using small scale specimens. The hysterisis loops, local buckling and failure modes are reported and discussed.

INTRODUCTION

Recent experimental investigations of the hysteresis behavior of steel bracing members include small scale tests on tubes with gusset plates by Jain (Ref. 1) and large scale testing of pin-ended and fully restrained members by Popov (Ref. 2). The test results were used to improve the multi-linear hysterisis models used in the dynamic analysis of building frames. The most significant result was that the effective slenderness ratio K ℓ/r governs not only the buckling load, but the entire hysterisis loop. However, because all these studies were restricted to axial loading only, the applicability of this concept to inclined restrained bracing members was not proven.

That failure of steel braces can contribute significantly to the earthquake damage was shown in the MIYAGI-KEN-OKI, Japan earthquake of June 12, 1978. This shows that there is a need for more full scale testing and to develop more rational design procedures for bracing members and their connections.

TEST PROGRAM

Test Equipment. The loading system (Fig. 1,2) consists of a reaction frame, a four hinge frame with the inclined specimen and the hydraulic actuator. The actuator capacity of 250 kips (1.1MN) allows to test sections from A36 steel of an area up to 6 in^2 (40 cm^2).

The axial displacement is measured separately on two telescoping rods. The average output of the two transducers is used as the controlling variable of the feedback system. The transducer for the lateral displacement is mounted on a bracket attached to the telescoping rods. The potentiometric transducers have a stroke of 6 or 12 in. (15 and 30 cm). The

---

I Doctoral canditate in Civil Engineering, Univ. of Michigan, Ann Arbor, Mich., USA

II Professor of Civil Engineering, Univ. of Michigan, Ann Arbor, Mich. USA

load is measured by the load cell of the actuator. The hysterisis loops are directly displayed on an X - Y plotter and all the transducer outputs are recorded on paper tape with a digital data acquisition system.

Specimens. The designation and geometry of the specimens are listed in Fig. 6. Three structural tubes and one wide-flange section were included in this first test series. All the specimens were fully welded to heavy end plates which were bolted to the frame with friction connections. The members were oriented to buckle in the plane of the frame.

The material properties obtained from coupon tests are summarized in Fig. 7. Whereas the wide-flange sections conformed to hot-rolled A36 steel, the tubes exhibited a lot of cold-work. However, because such members are typically used in building frames, they were tested as delivered.

Deflection history. The deflection history is shown in Fig. 5. The axial displacement is expressed in fictitious axial ductilities calculated for a yield strength of 36 ksi (248 MPa). The displacements are not normalized to the actual yield strength of the material. The purpose of sequence 0 is to straighten the specimen. Sequences 1 to 4 consist of a similar deflection pattern with increasing maximum contractions, which allows convenient interpretation of the fatigue behavior. Part A, where the same cycle is repeated in successive sequences, is used to study the deterioration of the hysterisis loops. Part B gives information about the maximum compressive load. It should be noted that the deflection history is given in absolute displacements and not reset after the yield load has been reached as in previous work (Ref. 1).

RESULTS AND INTERPRETATION

Mode of deflection. Considerable antisymmetric lateral displacement components were observed before the maximum compressive load was reached the first time. Afterwards the symmetric part took over and plastic hinges formed successively at midspan and at the ends (Fig. 2). The direction of buckling was determined by the sense of the initial crookedness.

Buckling load. For plotting the buckling load versus the effective slenderness ratio (Fig. 8), a K value of 0.5 was assumed corresponding to the hinge location. All the data points for first buckling are lying within limits found from an extensive study of column buckling. Except for test TW1 the results fit the European multiple column curves very closely. The measured initial crookedness (Fig. 6) is close to $\ell/1000$ which was used in the deviation of these curves. It is not known if the initial straightening increased the buckling load, because the beneficial effect of smaller initial crookedness might get cancelled by softening of the material due to the Bauschinger effect (Ref. 2). The agreement with the AISI curve is fair for the tubular members. However, it is known, that the AISC formula overestimates maximum loads for weak axis buckling of wide-flange shapes.

Hysterisis loops. Selected axial force versus displacement plots are shown in Fig. 10 to 13. The decrease in tensile strength for a cycle

with fixed deflection limits is considerable (Fig. 10). However, the tensile strength can be regained by increasing the axcial displacement (Fig. 10 to 13). The maximum compressive strength of the straightened member on the other hand is always decreasing in successive cycles (Fig. 8) and the increase of load by straightening is very limited (Fig. 11-13). The decrease in compressive strength is caused by the Bauschinger effect.

Lateral deflections. The plots of the lateral deflection at midspan versus the axial displacement (Fig. 10 to 13) show that a member becomes less and less straight for the same tension yield load. The relationship between the two displacements has a fairly constant, approximately parabolic shape which is explained by the compatibility condition in axial direction (Fig. 10). When the member yields this curve is translated along the axial displacement axis by an amount corresponding to the inelastic elongation. Because they were not yielded as much as the wide-flange shape, this effect is not as pronounced in the results of the tubes. Because the lateral displacement is mainly a geometric phenomena, it is similar for all the specimens.

Local buckling. Local buckling in the compression elements of the plastic hinges (Fig. 3) was observed in all tests. The buckles were generally most severe in the center because the connection plates limited the distortion of the cross-section at the ends. Upon straightening the members the buckles disappeared and had apparently no effect on the maximum tension load. Although the width-thickness ratios b/t (Fig. 6) meet the AISC requirements (Ref. 4) for compact sections (Fig. 7), local buckling cannot be prevented for such large inelastic cyclic strains. However, the formation of the buckles is delayed and the depth of the bulges decreases with decreasing b/t ratio (Fig. 9).

Fatigue cracks. All the tubes failed by the formation of a crack (Fig. 4) in the corner of the compression element of the center hinge. The growth of the crack could be observed in compression but the members failed only when the tension yield load was approached in the last cycle of a sequence. The life of the tubes increased with increasing slenderness ratio (Fig. 9) as observed by Jain (Ref. 1). The wide-flange shape failed by cracking at the tips of the weld to the end plates. The cracks are attributed to the fact that the weld was not continued around the tips of the flanges. This example shows that the life of a brace can be reduced by the connection performance.

CONCLUSIONS

Following conclusions can be drawn from the limited test results presented in this paper:

1. The inclination of the brace does not affect the hysterisis behavior to any significant extent. A K-value of .5 therefore can be used in the calculation of the effective slenderness ratio for these members.

2. Local buckling occurred in all members even if requirements for a compact section were met. However, the time of occurrence of the local buckles in the deflection sequence as well as their intensity depended

strongly on the width-thickness ratio.

3. The life of a specimen up to cracking increases with the slenderness ratio and is larger for the wide-flange sections than for the tubes. However, details of the connection design and fabrication can have a pronounced effect on the fatigue life of a bracing member.

ACKNOWLEDGMENTS

The research presented in this paper was jointly sponsored by the National Science Foundation (Grant No. ENV 76-82209) and the American Iron and Steel Institute (Project 301). The most generous help of Mike Johnson, graduate student in Civil Engineering at the University of Michigan, is greatly appreciated.

REFERENCES

1. Jain, A. K., Goel, S.C. and Hanson, R.D., 1978, "Inelastic Response of Restrained Steel Tubes," J. Str. Div., ASCE, Vol. 104, pp. 897-910.

2. Popov, E. P., 1979, "Inelastic Behavior of Steel Braces under Cyclic Loading," Proceedings, U.S. National Conference on Earthquake Engineering, EERI, Stanford, California, August.

3. Johnston, B. G., 1976, "Guide to Stability Design Criteria for Metal Structures," John Wiley & Sons, Inc., New York, N.Y.

4. American Institute of Steel Construction, 1978, "Specification for the Design and Fabrication of Structural Steel for Buildings," New York, N.Y.

5. Sherman, D.R., 1976, "Tentative Criteria for Structural Applications of Steel Tubing and Pipe," American Iron and Steel Institute, Washington, D.C.

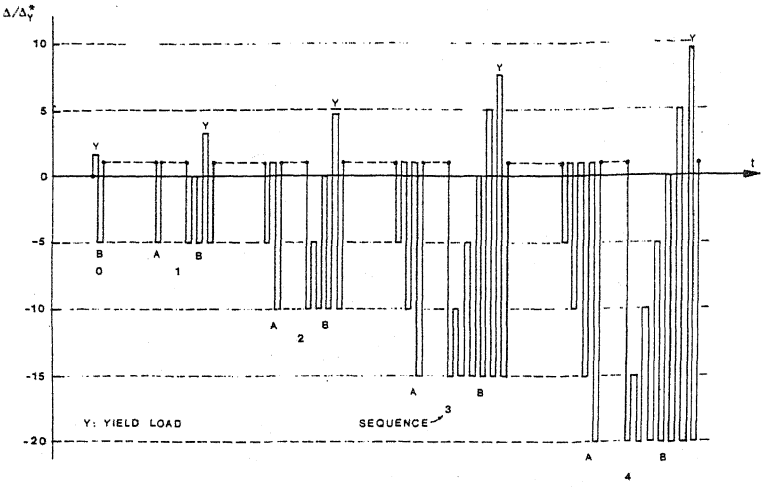

Fig. 5.
Deflection History
$\Delta y^* = .170$ in. (.432 cm)

Test	Section	Area $in^2(cm^2)$	ℓ/r	Max. b/t	v/ℓ
TW1	TS $7x5x\frac{1}{4}$	5.54(35.7)	71	27	-
TW2	TS $5x3x\frac{1}{4}$	3.54(22.8)	119	19	0.0013
TW3	TS $4x2x\frac{1}{4}$	2.59(16.7)	183	15	0.0013
WW1	W 10x15	4.41(28.5)	174	Web: 41 Flange: 8	0.0013

Length: 141"(358cm)

Fig. 6.
Designation of Specimens, Geometric Properties.

Sections	Material	Yield Strength ksi(MPa) [1]	Tensile Strength ksi [1]	Ultimate Strain % [1]	b/t for Compact Sections [2]
Structural Tubes	A500B	55(380)	64(440)	36	28
Wide-Flange	A36	47(320)	63(430)	35	Web: 32 Flange: 9

1) Average from 2-in gage length standard specimens.
2) AISC-Specification (Ref. 4) using minimum yield strength.

Fig. 7.
Material Properties and Required b/t Ratios For Compact Sections.

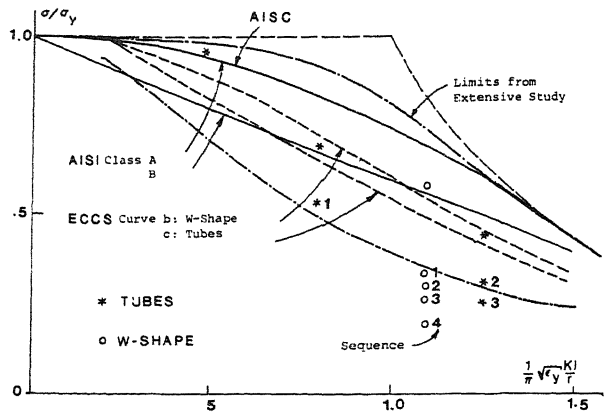

Fig. 8.
Test Results of Maximum Compressive Load Compared to Data from Ref. 3, 4 and 5.

Specimen	Local Buckling Sequence	Crack	
		Location	Sequence
TW1	during 1	corner of compression element, midspan	end of 2
TW2	during 2	do.	end of 3
TW3	during 4	do.	end of 4
WW1	during 3	tips of welds to end plates	end of 5

Fig. 9.
Local Buckling and Formation of Cracks

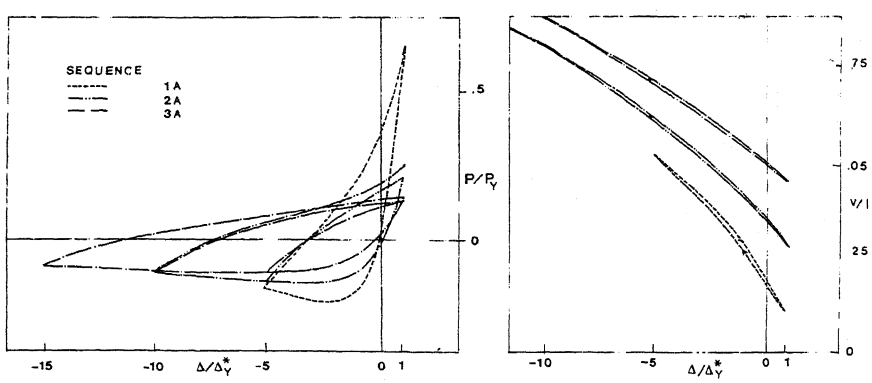

Fig. 10. Hysterisis Loops and Lateral Deflection, Part A of Deflection Sequence, Wide-Flange Section WW1, ℓ/r = 174, P_y = 210 kips (1.45 MN).

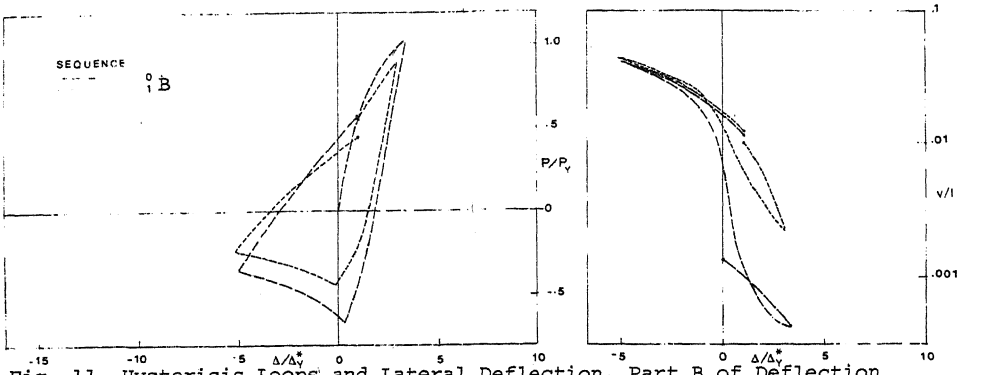

Fig. 11. Hysterisis Loops and Lateral Deflection, Part B of Deflection Sequence, Tube TW2, ℓ/r = 119, P_y = 195 kips (1.34 MN).

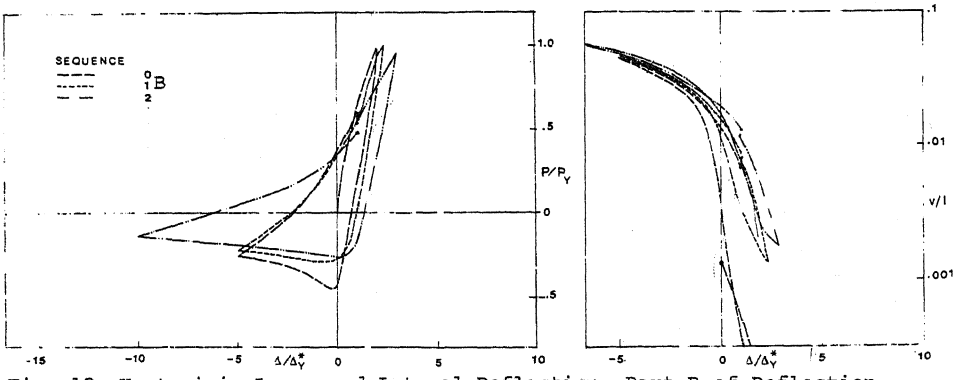

Fig. 12. Hysterisis Loops and Lateral Deflection, Part B of Deflection Sequence, Tube TW3, ℓ/r = 183, P_y = 140 kips (.98 MN).

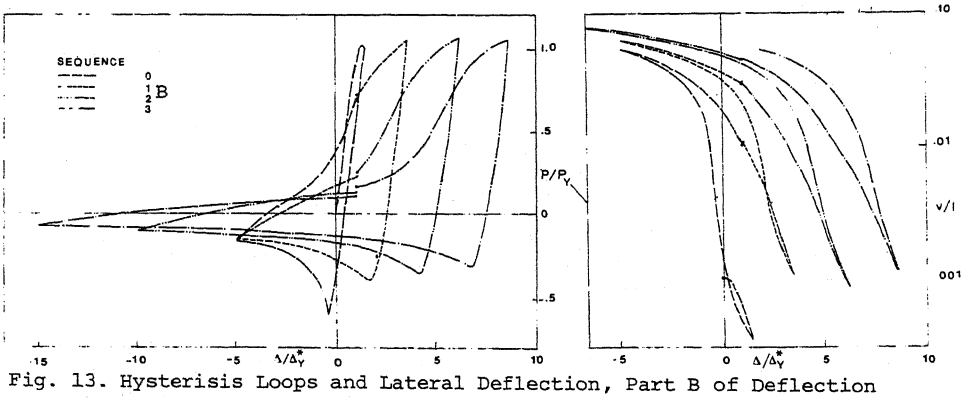

Fig. 13. Hysterisis Loops and Lateral Deflection, Part B of Deflection Sequence, Wide-Flange Section WW1, ℓ/r = 174, P_y = 210 kips (1.45 MN).